Acute Dosimetry and Estimation of Threshold Inducing Behavioral Signs of Thermal Stress in Rabbits at 2.45-GHz Microwave Exposure

Akimasa Hirata, *Member, IEEE*, Masami Kojima, Hiroki Kawai, *Member, IEEE*, Yoko Yamashiro, Soichi Watanabe, ,*Member, IEEE*, Hiroshi Sasaki[2], Osamu Fujiwara, *Member, IEEE*

***Abstract*—In the current international guidelines and standards for human exposure to microwaves, the basic restriction is determined by the whole-body average specific absorption rate (SAR). The basis for the guidelines is the adverse effect such as work stoppage in animals for whole-body average SARs above a certain level. Although it is known that absorbed microwave energy causes the behavioral sign of thermal stress, the relationship of whole-body average SAR with temperature/temperature elevation has not been sufficiently investigated. In the present study, we performed experiments on rabbits exposed to 2.45-GHz microwaves. A total of 24 measurements were conducted for power densities from approximately 100 to 1,000 W/m^2. Our computational code for electromagnetic-thermal dosimetry was used to set the exposure time duration and incident power density. Our experimental results suggest that a core temperature elevation of 1^{o}C is an estimate of the threshold inducing complex behavioral signs of microwave-induced thermal stress in rabbits for different whole-body average SARs and exposure time durations. The whole-body average SAR required for microwave-induced behavioral sign in rabbits was estimated as approximately 1.3 W/kg for 2.45-GHz microwaves.**

***Index Terms*— Biological effects of electromagnetic radiation, core temperature elevation, whole-body averaged specific absorption rate (SAR), bio-heat equation, human safety**

I. Introduction

THERE has been increasing public concern about the adverse health effects of human exposure to electromagnetic waves. In the microwave (MW) regions, elevated temperature (1^{o}C-2^{o}C) resulting from energy absorption is known to be a dominant cause of adverse health effects, such as heat exhaustion and heat stroke [1]. Microwaves of relatively low intensity absorbed in thermosensitive neural tissue have the potential to provoke immediate and dramatic changes in thermoregulatory effector response systems [2]. In safety guidelines and standards [3, 4], the whole-body average specific absorption rate (SAR) is used as a metric of human protection against MW exposure. The threshold whole-body average SAR is 4 W/kg. According to the ICNIRP guidelines [3], this threshold is based on the fact that laboratory animals exposed to MW of at least 4-8 W/kg exhibit a characteristic pattern of thermoregulatory behavior [5]. In addition, at SAR values in the range of 1–3 W/kg, rats and monkeys show decreased task performance [2, 6, 7]. The rationale of the IEEE standard [4] is based on behavioral effects (work stoppage) in rodents and non-human primates for about 1 hour at the threshold SAR (4 W/kg) associated with temperature elevation.

For humans, SAR and temperature elevation for MW exposures have been reported [8, 9]. Even though the limit for public environment in the safety guidelines is not applied [10], some studies have discussed the SAR compliance for medical devices [11, 12]. Typical scenarios for microwave whole-body exposures also include workers near base-station antennas of wireless communications and broadcasting transmitters [13]. The human volunteer studies have demonstrated that exposure for up to 30 min, under conditions in which whole-body SAR was less than 4 W kg, caused an increase in the body core temperature of less than 1°C [3].

Animal studies for the whole-body exposures referenced in international guidelines were conducted in the 1970s and 1980s [2, 5, 6, 7, 14]. Although characteristic patterns of thermoregulatory behavior were observed in animals, the relationship between the whole-body SAR and core temperature elevation was not well quantified. One reason for this limitation is that experimental and computational dosimetric techniques have not been well established until recently. In addition, laboratory rodents were employed in most of the above studies [5, 6, 7, 14, 15]. However, since rodents are small and have limited physiological heat loss mechanisms, they are poor models for human beings [16]. Ebert *et al.* recently investigated thresholds for thermophysiological responses and thermal breakdown for mice with respect to the whole-body average SAR [15].

In these circumstances, the questions arise whether *i)* the threshold depends on the species, and *ii)* the behavior is induced by temperature or temperature elevation. As for *i)*, the

Manuscript received May 25, 2009This work was supported in part the KDDI Foundation and Grant-in-Aid for Young Scientist (B), Japan..

A. Hirata, H. Sugiyama, and O. Fujiwara are with the Nagoya Institute of Technology, Nagoya 466-8555 Japan (e-mail: ahirata@nitech.ac.jp).

M. Kojima, Y. Yamashiro, and H. Sasaki are with Kanazawa Medical University, , Japan.

H. Kawai and S. Watanabe are with the National Institute of Information and Communications Technology, Tokyo 184-8795, Japan.

threshold for thermoregulatory behavior is 1.0 W/kg for rats [6] and 1.1 W/kg for squirrel monkeys [2]. One study [15] determined that the thermoregulatory system of mice can compensate for the absorbed energy and achieve a stable condition at 2-5 W/kg.

As for *ii)*, several studies on similar topics have been reported. Cell death or degeneration is reportedly caused by a temperature above 41°C-42°C for a specific time duration [17]. The temperature above a "set" temperature is said to cause thermoregulatory behavior [12]. Moreover, temperature elevation of 0.3°C in the hypothalamus by an implanted thermode was found to cause a thermoregulatory response [2]. In computational modeling, body temperature elevation is a factor influencing vasodilatation (e.g., [18], [19]).

The purpose of the present study is to perform an experiment involving rabbit exposure to 2.45-GHz MW far-fields to clarify the relationship between whole-body average SAR and the rectal temperature elevation in rabbits. The main reason for choosing rabbits is their high susceptibility to heat stress, since they have few sweat glands, and experience difficulty in eliminating excess body heat [20]. Thus acute dosimetry in a low heat tolerance animal experiment would provide useful information. The threshold for inducing a behavioral sign due to MW-provoked thermal stress is roughly estimated. Our attention here is not on the early phase of the thermophysiological response, in which an increase in blood volume due to movement of fluid from the extracellular space into the circulation would serve to increase heart rate and intraventricular blood pressure [3], but rather the complex behavioral sign related to thermal stress. This is because the rabbits are fixed in a plastic restrainer in order to conduct acute dosimetry, and thus proper thermoregulatory behavior and the early phase of the thermal response may not be observed. We determined the experimental conditions with our computational code for electromagnetic-thermal dosimetry [19].

II. METHODS

A. Animal Handling

The rabbits used in our experiment were cared for and handled in accordance with the Guidelines for Animal Experiments of Kanazawa Medical University. The average weight of young adult male pigmented rabbits is 2.0 kg (±10%). During exposure, a pigmented rabbit was immobilized in a polycarbonate rabbit holder [21]. In the present study, holes were made in the holder to maximize the heat transfer between air and skin. In the control case without MW exposures, the rectal temperature variation of the rabbit due to insertion for 30 min or more in the holder was confirmed to be marginal. This is because the heat transfer between air and skin excluding ear lobe is not a dominant factor in the thermal balance of rabbits [20]. Basal metabolism and vasomotor adjustment are reportedly factors [16].

To investigate the effect of anesthesia on the core temperature elevation and thermophysiological response, some rabbits were exposed to ketamine hydrochloride (5 mg/kg)+ xylazine (0.23 mg/kg) injected intramuscularly. Note that the administration of anesthesia reduces the blood perfusion and basal metabolic rate together with inactivating the thermoregulatory response [21, 22, 23]. Not all rabbits were exposed to anesthesia.

B. Experimental Condition

The experiment was conducted in the anechoic chamber (10 m × 8 m × 6.5 m). Air temperature was kept at 21°C-24°C by an air conditioner. The humidity during the experiment ranged from 28% to 31%. This condition is classified as 'absence of heat stress' [20]. The chamber is sufficiently large so that wind from the air conditioner does not reach a rabbit directly. For measuring the core temperature, a flexible thermal probe (1.6 mm in diameter) was inserted 100 mm into the rectum. A fluoroptic thermometer (Anritsu FL-2000, Tokyo) was calibrated using a standard thermometer. The resolution of the probe was 0.1°C measured at intervals of 10 s.

In addition to the rectal temperature, the eye temperature was measured as in our previous study [21]. Temperatures of the eye segments were measured with a Fluoroptic thermometer (Luxtron 790, Luxtron, Santa Clara, CA) according to the following procedure: each rabbit eye was anesthetized with a 0.4% oxybuprocaine hydrochloride ophthalmic solution applied as eye drops; thermometer probes (0.5 mm in diameter) were then inserted into the lens nuclear part. Note that a guide hole for the temperature probe was made using a 20-gauge injection needle at 12 o'clock of pars plana. The thermo-probe was inserted into the hole, and the thermo-sensor part was fixed in the center of the pupillary area. The thermo-probe and eyeball were fixed with super glue at 12 o'clock. These procedures were performed under slit lamp microscope observation [21]. The tip of the thermo-probe was set on the optical axis in the center of the pupillary zone and measured at one-second intervals. In the thermal modeling, there are many thermal parameters. The simultaneous measurement at different points, especially core and local temperatures, serves to validate our computational modeling.

C. Experimental Setup

We used two different MW sources to realize different incident power densities. A rabbit was irradiated from the lateral side to maximize the whole-body average SAR at the same incident power density. The MW frequency was 2.45 GHz. The experimental setup is summarized in Fig. 1.

For incident power densities of 110 and 220 W/m^2, the exposure system was the same as reported earlier in [19]. A double-ridged waveguide horn antenna (Model 3115, ETS-LINDGREN Inc., Cedar Park, TX) was used for the exposure. The 1-m distance between the rabbit and antenna was chosen so that fields radiated from the antenna were considered as far-fields. The signal generated in an electric signal generator (E4438C-402, Agilent Technologies, Santa Clara, CA) was amplified via a power amplifier (TWAL 0208-250, Bonn Elektronik Inc., Ottobrunn, Germany). Antenna power was monitored with a power sensor (Agilent, 8481A)

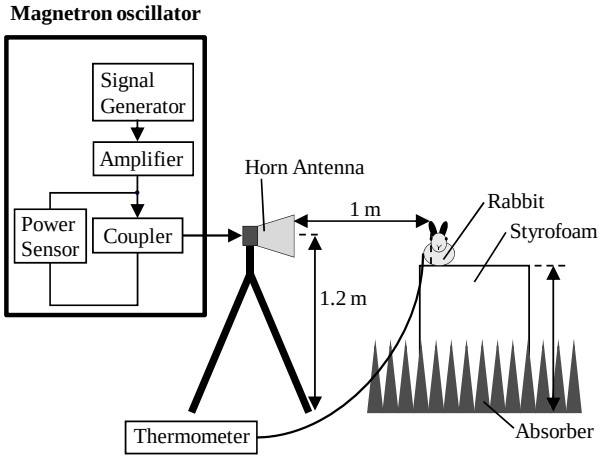

(a)

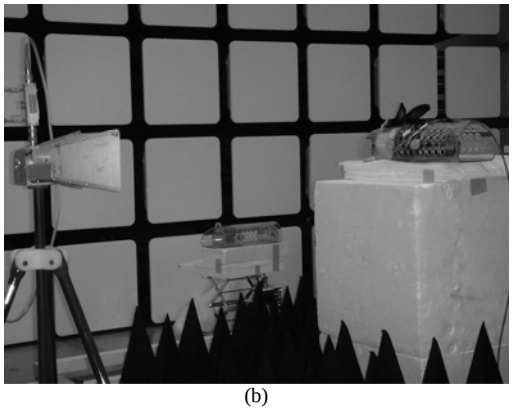

(b)

Fig. 1. (a) Diagrammatic representation of the exposure system, and (b) a

throughout the measurement.

For incident power densities of 730 and 980 W/m^2, a waveguide horn antenna (WAN-021-20, Nihon Koshuha Co., Ltd., Yokohama, Japan) and a magnetron oscillator (Nihon Koshuha, MKN-156-3S2A) were used. As shown in Fig. 1, the magnetron oscillator is comprised of a generator, amplifier and power sensor. The 1.2-m distance between the rabbit and antenna was chosen for the same reason as the system for lower power densities.

Since we used horn antennas, the radiated fields cannot be considered as a plane wave. To estimate the effective power incident to a rabbit, we measured the electric field in the region of a rabbit using a probe with a resolution of 50 or 100 mm [17]. The corresponding average power density was defined as the incident power density. This average power is expected to be acceptable since the reference levels in the ICNIRP guidelines [2], which establish the field or power density for practical exposure assessment, are intended to be spatially averaged values over the entire body of the exposed individual.

D. Numeric Rabbit Phantom

We developed an anatomically-based rabbit phantom with a resolution of 1 mm. This was constructed on the basis of X-ray CT images taken at Kanazawa Medical University, Japan [24]. This model was comprised of 12 types of tissue: skin, muscle, bone, fat, brain, cerebrospinal fluid, anterior chamber, vitreous, retina/choroid/sclera, iris/ciliary body, lens, and cornea. Specifically, the model thicknesses become largest around the optic nerve head. In our model, the retina/choroid/sclera is further classified into two parts on the basis of blood perfusion. More detailed information of the tissue classification can be found in our previous studies [24, 25]. The width, depth, and height of the model were 123 mm, 260 mm, and 152 mm, respectively. The weight of the rabbit phantom was 2.5 kg. To match the average weight of rabbits employed in this study and that of the phantom, we linearly reduced the cell size of the rabbit phantom from 1 mm to 0.93 mm.

E. SAR Calculation

The finite-difference time-domain (FDTD) method [25] is used to investigate MW power absorbed in the rabbit phantom. For truncation of the computational region, we adopted perfectly matched layers as the absorbing boundary. To incorporate the rabbit model into the FDTD scheme, the dielectric properties of tissues were required. These were determined with the 4-Cole-Cole extrapolation [26].

For harmonically varying fields, the SAR is defined as

$$\mathrm{SAR} = \frac{\sigma}{2\rho}|\hat{E}|^2 = \frac{\sigma}{2\rho}(|\hat{E}_x|^2 + |\hat{E}_y|^2 + |\hat{E}_z|^2) \quad (1)$$

where $\hat{E}_x$, $\hat{E}_y$, and $\hat{E}_z$ [V/m] are the peak values of the electric field components, σ and ρ, which denote the conductivity and mass density of the tissue, respectively.

F. Temperature Calculation

Our formula for the temperature calculation was presented in our previous study [19]. In that study, we applied an active blood perfusion model of humans [18, 27] to rabbits, together with a parametric study. The sweat glands in rabbits are virtually nonfunctional, allowing us to neglect this mechanism in our modeling. During heat stress, rabbits try to sustain homeothermy by using internal physiological measures [20], such as changes in breathing rates and peripheral (ear) temperatures. In our measurement, increased breathing rates, together with nose licking, were observed. It is beyond the scope of our study to develop a model for such responses in our computation, since the main purpose of the present study is to estimate thresholds for such behavioral signs of MW-induced stress.

Bioheat Equation

The bioheat equation is used to calculate temperature elevations in the rabbit model [28]:

$$C(\mathbf{r})\rho(\mathbf{r})\frac{\partial T(\mathbf{r},t)}{\partial t} = \nabla\cdot(K(\mathbf{r})\nabla T(\mathbf{r},t)) + \rho(\mathbf{r})SAR(\mathbf{r}) + A(\mathbf{r}) - B(\mathbf{r},t)(T(\mathbf{r},t) - T_B(t)) \quad (2)$$

where $T(\mathbf{r},t)$ [°C] and $T_B(t)$ [°C] denote the respective temperatures of tissue and blood, C is the specific heat of tissue, K is the thermal conductivity of tissue, A is the basal metabolism per unit volume, and B is the term associated with

blood flow. Thermal parameters used in our modeling are the same as listed in [19] for unanesthetized rabbits. Before exposure, the basal metabolism and heat transfer from the body to the air get balanced for a given set of parameters. When rabbits were anesthetized, the basal metabolic rate was reduced by 30-35% [23]. This reduction ratio was estimated not for specific tissues or body parts but over the whole body. The blood perfusion rate and metabolic rate are roughly proportional to each other [28]. Thus, the blood perfusion rate and basal metabolic rate of each tissue are considered to be reduced by 30% compared with those of unanesthetized rabbits.

The blood temperature is assumed to be constant over the whole body, since the blood circulates throughout the human body in one minute or less. In rabbits, it takes far less time because of their smaller dimensions and higher blood perfusion rate. The boundary condition between air and rabbit tissue for (2) is given by the following equation:

$$-K(r)\frac{\partial T(\mathbf{r},t)}{\partial n} = h\cdot(T_s(\mathbf{r},t)-T_e(t)) \tag{3}$$

where h [W/m^2/^{o}C], T_s [^{o}C], and T_e [^{o}C] denote, respectively, the heat transfer coefficient, surface temperature, and air temperature. The heat transfer coefficient h is given by the summation of radiative heat loss h_{rad}, convective heat loss h_{conv}, and evaporative heat loss h_e. The respective values of the heat transfer coefficients between the skin (excluding the ear lobe) and air, between the internal air and tissue, and between the ear lobe and air are 0.65 W/m^2/^{o}C, 13 W/m^2/^{o}C, and 2.5 W/m^2/^{o}C, respectively [19].

The bioheat equation is particularly effective in the shallow region of the body, where modeling the vasculature system is not required. In other words, the temperature calculated becomes unreliable in proportion to the distance from the body surface. However, the MW power absorption or heat source is concentrated around the surface in a 2.45-GHz exposure system, since the penetration depth of the MW is a few centimeters. Hence, the body-core temperature elevation is mainly caused by the circulation of temperature-elevated blood. The calculation scheme for the blood temperature is thus essential in the computational modeling. The blood temperature changes according to the following equation to satisfy the thermodynamic laws [22, 30, 31]:

$$T_B(t) = T_{B0} + \int_t \frac{Q_{BTOT}(t)}{C_B\rho_B V_B}dt \tag{4}$$

$$Q_{BTOT}(t) = \int_V B(t)(T_B(t)-T(\mathbf{r},t))dV \tag{5}$$

where Q_{BTOT} [W] is the rate of heat acquisition of blood from body tissues. C_B (=4000 J/kg$\cdot^\circ$C), ρ_B (=1050 kg/m^3), and V_B denote the specific heat, mass density, and total volume of blood, respectively. Note that the average blood volume per unit rabbit body mass is 56 ml/kg. The blood volume is set at 110 ml, since the weight of our rabbits is 2.0 kg on average.

Thermophysiological Response

For temperature elevation above a certain level, blood perfusion is activated to carry away the excess heat produced. As for blood perfusion for all tissues except the skin, the regulation mechanism is governed by the local tissue temperature. When that temperature remains below a certain level, blood perfusion is equal to basal value B_0. Once the local temperature exceeds a given threshold, the blood perfusion increases almost linearly with the temperature to carry away the heat evolved [27].

The variations of blood perfusion in the skin through vasodilatation are expressed as the temperature increase in the hypothalamus and the average temperature increase in the skin [26, 30]. These thermophysiological responses have been taken into acount in our computational modeling.

G. Dosimetric Scenarios

A rabbit is irradiated from the lateral side to maximize the whole-body average SAR for a given incident power density. The whole-body average SAR for the incident power density of 100 W/m^2 has been computed as 1.18 W/kg [19]. Based on this result, the whole-body average SAR for different power densities can be scaled linearly. Using two experimental setups, we chose incident power densities of 980, 730, 220, and 110 W/m^2.

For an incident power density below a certain level, a rabbit is expected to compensate for the heat load due to MW absorption by increasing breathing rates and/or adjustment of its basal metabolism [2]. A heat transfer coefficient between internal tissue and air for rabbits with increased breathing rate due to heat load was derived in our previous study [19]. Then, the incident power density of 110 W/m^2 was derived so that the MW energy and heat transfer from rabbit to air became identical for the heat transfer coefficient considering the increased breathing rate. In our computation, the plane wave was incident to the rabbit model instead of the non-uniform fields mentioned in Sec. II C.

III. Results

An immobilized rabbit was exposed to 2.45-GHz MW radiated by the double-rigged antenna, as shown in Fig. 1. The duration was determined based on our computational code so that the core temperature elevation did not exceed 1.5^{o}C. The main aim of the present study is to conduct acute dosimetry for high thermal loads due to MW energy.

The experiment was first conducted on anesthetized rabbits for ethical reasons. After confirming the validity of our computational code for anesthetized rabbits, the duration of exposure for unanaesthetized rabbits was determined. When the core temperature of a rabbit without MW exposure was higher than 40^{o}C, the exposure was terminated at 41.5^{o}C. We made 24 measurements, 10 on anesthetized and 14 on unanesthetized rabbits.

In our computation, first, the temperature distribution in the rabbit without MW energy was calculated by substituting the room temperature and blood (or rectal) temperature. Then, the temperature distribution for MW exposure was calculated by substituting SAR obtained by the electromagnetic solver into the bioheat equation. The temperature elevation distribution is

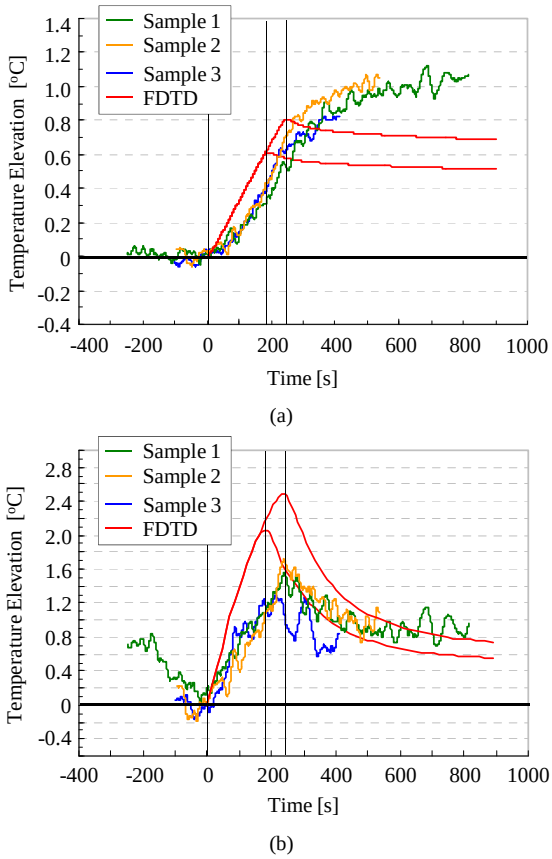

Fig. 2. Temperature elevations in (a) rectum and (b) eye lens of rabbit. Incident power density was 1,000 W/m^2. Subjects 2 and 3 are anesthetized, but not Subject 1.

defined as the difference between the temperature distribution with and without MW exposure. Different thermal parameters of rabbit tissue were used for the cases with and without anesthesia. Even though different rectal and blood temperatures are used in our computation, no clear difference was observed in core temperature. Thus, the room and blood temperature are assumed to be 25°C and 39.5°C, respectively, for the computational results presented in Figs. 2 and 3.

A. Comparison of Computed and Measured Temperature Elevation in Rabbits

In this subsection, we present the time course of temperature elevations at incident power densities of 980 and 110 W/m^2. Figure 2 shows the temperature elevations in the (a) rectum and (b) eye lens of rabbits at the incident power density of 980 W/m^2. Rabbits 1 and 2 were anesthetized but not Rabbit 3. The duration of the exposures was 4 minutes for the rabbits with anesthesia and 3 minutes for the rabbits without it. As shown in Fig. 2 (a), the measured core temperature elevates slower than the computed ones. The measured core temperature continued to elevate after the exposure was terminated. However, the maximum temperature elevation was reasonably estimated with the computational code. No clear differences were observed between temperature variations with and without the anesthesia. A similar tendency was observed for the incident power density of 220 W/m^2 [18]. As shown in Fig. 2 (b), the measured

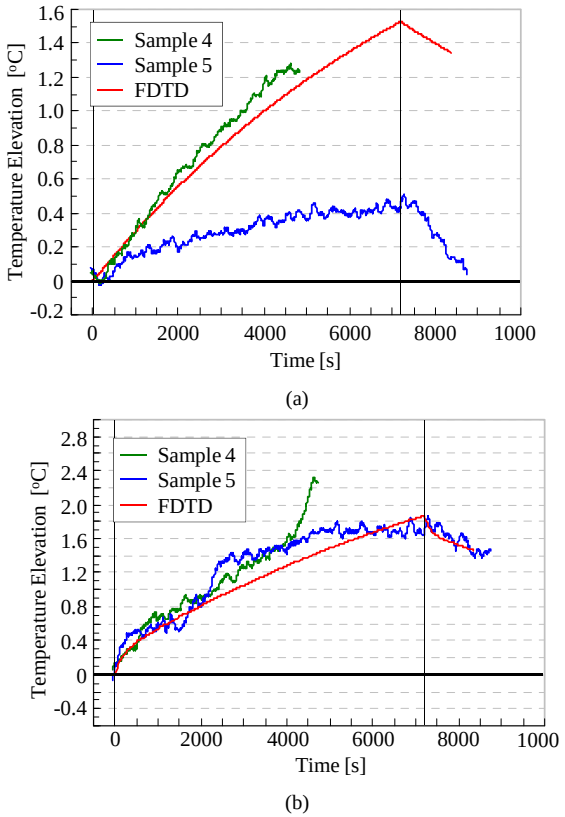

Fig. 3. Temperature elevations in (a) rectum and (b) eye lens of rabbit. Incident power density was 110 W/m^2.

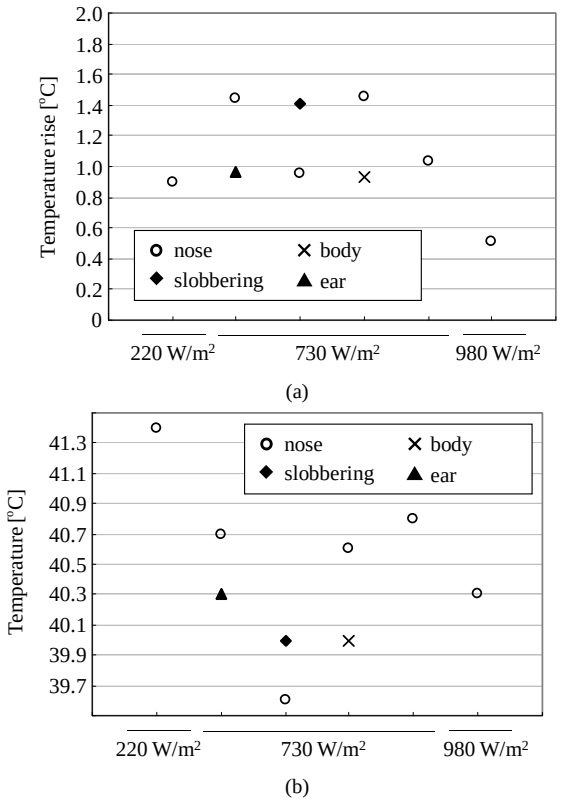

Fig. 4. Threshold temperature (a) and temperature elevation or (b) of rabbits at which the behavioral signs of thermal stress were observed. Nose, body, and ear represent licking the nose, movement in the plastic holder, and movement of ear lobe, respectively.

temperature in the eye does not elevate as much as that of the computed temperature. This difference is discussed in the next section. Note that the temperature in the lens before exposure is not stable unlike rectal temperature. One of the main reasons for perturbation is attributed to blinking which made the lens temperature vary by 1°C or more. Some abrupt change in the lens during exposure is also attributed to blinking. Figure 3 shows the temperature elevations in rabbits for the incident power density of 110 W/m^2. For this incident power density, only rabbits without anesthesia were considered. The reason for this is that the core temperature elevation in rabbits with anesthesia becomes comparable to the temperature decrease due to the lowered basal metabolism [19]. In addition, because the duration of anesthesia is generally less than 30 minutes, we could not investigate the temperature elevation properly for such an anesthetized rabbit with more than 30 minutes of exposure. In our experiment, the duration of exposure was determined as 120 min. As shown in Fig. 3 (a), good agreement was observed between computed and measured core temperature elevations for Rabbit 4 but not Rabbit 5. This difference for Rabbit 5 is due to the thermophysiological response, as expected. As shown in Fig. 3 (b), reasonable agreement was observed on the eye temperature elevations for both Rabbits. The difference between the computational and measured results is discussed in the next section.

B. *Estimation of Threshold Inducing Sign of Thermal Stress in Rabbits*

Among the 14 unanesthetized rabbits, complex behavioral signs due to thermal stress were observed in 6 rabbits. One of the possible reasons for rabbits not exhibiting such signs is thought to be the difference in the set temperature inducing the thermoregulation. No anesthetized rabbit exhibited such behavior. Their behaviors depend on the individual rabbit and include increased breathing rates, repetitive movement in the plastic holder, nose licking, slobbering and movement of the ear lobe. Figure 4 shows the threshold temperature and temperature elevation at which rabbits exhibit repetitive behaviors. As shown in Fig. 4 (a), the rectal temperature at which rabbits showed such behavior ranged from 39.6°C to 41.5°C, and was dependent on the individual rabbit. In contrast, the temperature elevation of 0.9°C-1.0°C seems to be the estimate of lower threshold for inducing a behavioral sign of thermal stress in rabbits. This estimated value of temperature elevation is comparable to 1°C, which corresponds to the international guidelines to prevent MW-induced excess temperature elevation in different species [1, 3, 4].

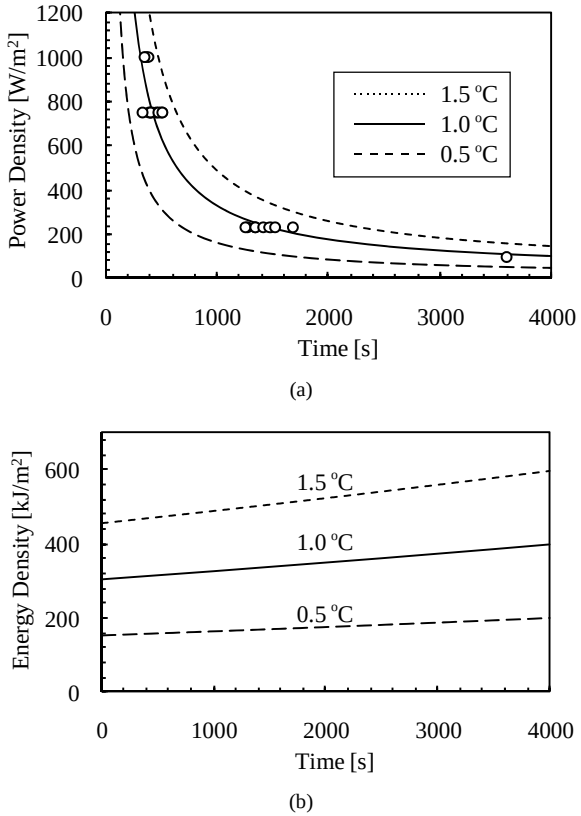

Fig. 5. Relationship between (a) incident power density / (b) incident energy density and exposure duration required for core temperature elevation of 1°C. Computational results for 0.5°C, 1.0 °C and 1.5°C are also plotted.

C. *Incident Power Density and Duration Required to Elevate Core Temperature of 1°C*

In Sec. III B, we showed that a temperature elevation of approximately 1°C is the threshold for inducing a behavioral sign of MW-induced thermal stress. Here, we use Fig. 5 to investigate the relationship between the incident power/energy density and duration of MW required to elevate the core temperature by 1°C. Note that this is the incident power density for rabbits exposed from the lateral side, which maximizes the whole-body average SAR. As shown in Fig. 5 (a), the incident power density for the core temperature elevation of 1°C decreases with the exposure duration. The measured temperature elevations are generally in agreement with the computed values. In Fig. 5 (b), the energy density required for the temperature elevation of 1°C gradually increases with the exposure duration. This increase of energy with time corresponds to the energy discharged from a rabbit's body during exposure. Rabbits are sensitive to heat stress [20], so they are unable to discharge much heat to the environment during the MW exposure. Thus, energy required to elevate core temperature is rather insensitive to the exposure duration. This figure suggests that the body core temperature elevation approximately represents energy stored in the body.

IV. Discussion

Let us discuss the difference between the computed and measured temperature elevations. In Fig. 2 (a), the difference in rectal temperatures is attributed to equation (4), in which the blood temperature is assumed to be spatially uniform over the body. In addition, the temperature was measured at the rectum, whereas the computed value represented blood. The rectal temperature elevation has been reported to be delayed compared to the blood temperature by a few minutes [31],

because it takes time to elevate the tissue temperature via the circulation of the blood of elevated temperature, together with non-uniformity of the blood temperature. The second reason for the difference in computed and measured temperatures is considered to be the increased metabolism [22], which may be caused by stress response due to the rapid temperature elevation. The third is due to the uncertainty of the basal metabolism/blood perfusion rate of tissues, which depends on the individual and body parts. Note that the blood perfusion rate and basal metabolism of tissues are proportional to each other [29]. In addition, the number of tissues considered in the rabbit is limited to 12 in our numeric phantom.

In Fig. 3, the measured core temperature elevation in Rabbit 4 is smaller than the computed value and becomes saturated. Let us discuss this difference in terms of the heat balance equation given in [15, 16]:

$$M + P_{MW} - P_{conv} = S \quad (12)$$

where M [W] is the rate at which thermal energy is produced through metabolic processes. P_{MW} [W] is the MW power absorbed in the body, P_{conv} [W] is the rate of heat exchange with convection, and S [W] is the rate of heat storage in the body. Regimes exist that compensate for P_{MW} by metabolic and vasomotor adjustments [15]. These adjustments correspond to the decrease of M and increase of breathing rates with temperature elevation, and so correspond to the increase of the value of P_{conv}. For the time course of the core temperature in Rabbit 5, we estimated the heat loss due to these mechanisms by assuming that the lowered basal metabolism or increased breathing rate compensates for the MW power absorption. From the computational results, the heat loss was estimated at 0.8 W/kg, corresponding to 20% of the basal metabolic rate. This reduction ratio coincides with that reported in [2] for squirrel monkeys.

Figure 4 suggests that, except for one rabbit, the temperature elevation of 0.9°C-1.1°C in the rabbit indicates a behavioral sign of MW-induced thermal stress, although the number of rabbits exhibiting the sign was limited. It should be noted that the threshold estimation would depend on the environmental condition including the restraint and behavioral sign and response monitored, etc. The difference in the behavioral sign even for the same incident power density is uncertain since the environmental condition is kept almost identical and the number of rabbits exhibiting the behavioral sign was limited. One of the possible reasons for this variability is the stress response of rabbits in the restrainer as mentioned above.

With an incident power density of 980 W/m^2, the computed skin temperature elevation was 3.0°C when the measured rectal temperature was 0.6°C. When the measured rectal temperature elevation was 1°C for the incident power density of 730 W/m^2, the computed skin temperature elevation was 2.4°C. This difference in skin temperature occurs because the thermoregulatory behavior of the rabbit at rectal temperature elevation is less than 1°C. A lower incident power density has been reported more often in the infrared region than in the MW region owing to skin heating [2], which would be primarily due to temperature elevation in the skin or the thermal sensation [32].

Even though power densities tested were limited to 110, 220, 730, and 980 W/m^2, the threshold incident power density inducing a complex behavioral sign was approximately 110 W/m^2, which corresponds to the whole-body average SAR of 1.3 W/kg. Since the difference in thresholds between thermoregulatory and breakdown regions is reportedly not much [14], we did not conduct further measurements with different power densities. Three main factors cause uncertainty in power density. One is the definition of incident power density, which was determined by averaging over the entire body of the exposed individual. The second is the fluctuation of 5%-10% in the power emitted from the oscillators, while the third is the difference of 5%-10% in the rabbit dimensions, although only the average weight of the rabbits was used in our computation. Even with such uncertainty, the threshold whole-body SAR causing behavioral sign of MW-induced thermal stress was in reasonable agreement with the thermoregulatory behavior reported [14]; 1.0 W/kg for rats [6] and 1.1 W/kg for squirrel monkeys [2]. In contrast, the thermoregulatory region was determined as 2-5 W/kg for mice [14] and 2 W/kg for rats [26]. The threshold for mice [14] may be comparable to our results in terms of the ratio of approximately 20% for the basal metabolic rate. In addition, the difference may be the restraint condition for the animals during the experiments. Furthermore, all mice were acclimatized and trained to the restrainer tube [12], although such were not done here since it is not common for rabbits.

V. Conclusion

In current international guidelines and standards [1, 2], the whole-body average SAR is the basis of exposure restrictions. In addition to human studies, animal studies, especially on rodents, are referenced in these guidelines and standards. The rationale for the guidelines is that characteristic behavioral thermoregulation is observed for the whole-body average SAR above a certain level [3]. Acute dosimetry in animals is highly useful for extrapolating the guidelines for humans and for confirming the scientific basis of current safety guidelines for human protection. However, the relationship between energy absorption and temperature elevation has not been stated in detail.

Twenty-four measurements were recorded for 2.45-GHz MW exposure at power densities from approximately 100 to 1,000 W/m^2. For the whole-body average SAR of 2.6 W/kg, the core temperature in rabbits elevates with time without becoming saturated. On the contrary, the temperature was elevated with time for one rabbit, but not for other rabbits at the whole-body average SAR of 1.3 W/kg. The SAR value of 1.3 W/kg for the behavioral sign of thermal stress is in reasonable agreement with thermoregulatory behavior in several previous studies [2, 6, 8]. One of the primary differences is due to the weak susceptibility of rabbits to heat stress [20], in addition to the differences in the basal metabolism and restraint condition of

the experimental animals. The calculated whole-body average SARs required to elevate body-core temperature elevation in a rabbit by 1°C were 2.3 and 1.3 W/kg for 30 min. and 1 hour against 6.7 and 6.5 W/kg, respectively, for humans for the same time durations [29]. The temperature elevation in humans becomes saturated within approximately one-half hour, since the heat in humans can become balanced due to perspiration, which is not possible in rabbits. These comparisons support the perception that humans have a thermoregulatory capability greater than other endotherms during MW exposure [2].

REFERENCES

[1] G. O. Young, "Synthetic structure of industrial plastics (Book style with paper title and editor)," in *Plastics*, 2nd ed. vol. 3, J. Peters, Ed. New York: McGraw-Hill, 1964, pp. 15–64.

[2] American Conference of Government Industrial Hygienists (ACGIH), Threshold limit values for chemical substances and physical agents and biological exposure indices (Cincinnati OH), 1996

[3] E. R. Adair and B. W. Adams, "Microwaves modify thermoregulatory behavior in squirrel monkey," *Bioelectromagnetics*, vol.1, pp.1-20, 1980.

[4] International Commission on Non-Ionizing Radiation Protection (ICNIRP), "Guidelines for limiting exposure to time-varying electric, magnetic, and electromagnetic fields (up to 300 GHz)," *Health Phys.*, vol.74, pp.494-522, 1998.

[5] IEEE C95.1. IEEE standard for safety levels with respect to human exposure to radio frequency electromagnetic fields, 3 kHz to 300 GHz. New York: IEEE, 2006.

[6] S. M. Michaelson, "Biological effects and health hazard of RF and MW energy; fundamentals and overall phenomenology," In: Biological effects and dosimetry of nonionizing radiation (M. Grandolfo, S. M. Michaelson, and A. Rindi, eds.) New York, Plenum Press, pp.337-357, 1983.

[7] S. Stern, L. Margolin, B. Weiss, S. Lu, S. M. Michaelson, "Microwaves effects on thermoregulatory behavior in rats," *Science*, vol.206, pp.198-201, 1979.

[8] J. A. D'Andrea, J. R. DeWitt, O. P. Gandhi, S. Stensaas, J. L. Lords, H. C. Neilson, "Behavioral and physiological effects of chronic 2450-MHz microwave irradiation of the rat at 0.5 mW/cm^2," *Bioelectromagnetics*, vol.7, pp.45-56, 1986.

[9] K. R. Foster and E. R. Adair, "Modeling thermal responses in human subjects following extended exposure to radiofrequency energy," *Biomed Eng. Online*, vol.3, 4, 2004.

[10] A. Hirata, T. Asano, and O. Fujiwara, "FDTD analysis of body-core temperature elevation in children and adults for whole-body exposure," *Phys. Med. Biol.*, vol.53, pp.5223-5238, 2008.

[11] Center for Devices and Radiologic Health, Guidance for the submission of paremarket notifications for magnetic resonance diagnostic devices. Rockville, MD: Food and Drug Administration (http://www.fda.gov/cdrh/ode/guidance/793.html), 1998.

[12] C. M. Collins, W. Liu, J. Wang, R. Gruetter, J. T. Vaughan, K. Ugurbil, M. B. Smith, "Temperature and SAR calculations for a human head within volume and surface coils at 64 and 300 MHz," *J. Magnet. Resonance Imag.*, vol.19, no.5, pp.650-656, 2004.

[13] K. Shiba, M. Nukaya, T. Tsuji, K. Koshiji, "Analysis of current density and specific absorption rate in biological tissue surrounding transcutaneous transformer for an artificial heat," *IEEE Trans. Biomed. Eng.*, pp.205-213, no.1, 2008.

[14] F. J. C. Meyer, D. B. Davidson, U. Jakobus, and M. A. Stuchly, "Human exposure assessment in the near field of GSM base-station antennas using a hybrid finite element/method of moments technique," *IEEE Trans. Biomed. Eng.*, vol.50, no.2, pp. 224-233, Feb 2003.

[15] S.-T. Lu, N. A. Lebda, S.-J. Lu, S. Pettit, S. M. Michaelson, "Effects of microwaves on three different strains of rats," *Radiation Res.*, vol.110, pp.173-191, 1987.

[16] S. Ebert, S. J. Eom, J. Schuderer, U. Spostel, T. Tillmann, C. Dasenbrock, and N. Kuster, "Response, thermal regulatory threshold of restrained RF-exposed mice at 905 MHz," *Phys. Med. Biol.*, vol.50, pp.5203-5215, 2005.

[17] E. R. Adair and D. R. Black, "Thermoregulatory responses to RF energy absorption," *Bioelectromagnetics Supplement*, vol.6, pp.S17-S38, 2003.

[18] F. C. Henriques Jr., "Studies of thermal injury, the predictability and the significance of thermally induced rate process leading to irreversible epidermal injury" *Arch. Pathol.*, vol.43, pp.489-502, 1947.

[19] R. J. Spiegel, "A review of numerical models for predicting the energy deposition and resultant thermal response of humans exposed to electromagnetic fields," *IEEE Trans. Microwave Theory Tech*, vol.32, no.8, , pp.730-746, 1984.

[20] A. Hirata, H. Sugiyama, M. Kojima, H. Kawai, Y. Yamashiro, O. Fujiwara, S. Watanabe, and K. Sasaki, "Computational model for calculating body-core temperature elevation in rabbits due to whole-body exposure at 2.45 GHz," *Phys. Med. Biol.*, vol.53, pp.3391-3403, 2008.

[21] I. F. M. Marai, A. A. M. Habeeb, and A. E. Gad, "Rabbits' productive, reproductive and physiological performance traits as affected by heat stress: a review," *Livestock Prod. Sci.*, vol.78, no.2, pp.71-90, Dec. 2002.

[22] M. Kojima, I. Hata, K. Wake, S. Watanabe, Y. Yamanaka, Y. Kamimura, M. Taki, and K. Sasaki, "Influence of anesthesia on ocular effects and temperature in rabbit eyes exposed to microwaves," *Bioelectromagent.*, vol.25, pp.228-233, 2004.

[23] E. R. Adair, B. W. Adams, G. M. Akel, "Minimal changes in hypothalamic temperature accompany microwave-induced alteration of thermoregulatory behavior," *Bioelectromagnet.*, vol.5, pp.13–30, 1984.

[24] A. Hirata, S. Watanabe, M. Taki, M. Kojima, I. Hata, K. Wake, K. Sasaki, and T. Shiozawa, "Computational verification of anesthesia effect on temperature variation in rabbit eyes exposed to 2.45-GHz microwave energy," *Bioelectromagnet.*, vol.27, pp.602-612, 2006.

[25] K. Wake, H. Hongo, S. Watanabe, M. Taki, Y. Kamimura, Y. Yamanaka, T. Uno, M. Kojima, I. Hata, and K. Sasaki, "Development of a 2.45-GHz local exposure system for in vivo study on ocular effects," *IEEE Trans. Microwave Theory & Tech.*, vol.55, no.3, pp.588-596, Mar. 2007.

[26] A. Taflove and S. Hagness, Computational Electrodynamics: The Finite-Difference Time-Domain Method: 2nd Ed. Norwood. MA: Artech House, 1995.

[27] C. Gabriel, Compilation of the dielectric properties of body tissues at RF and microwave frequencies. Final Tech Rep Occupational and Environmental Health Directorate. AL/OE-TR-1996-0037 (Brooks Air Force Base, TX: RFR Division), 1996.

[28] M. Hoque and O. P. Gandhi, "Temperature distribution in the human leg for VLF-VHF exposure at the ANSI recommended safety levels," *IEEE Trans. Biomed. Eng.*, vol.35, no.6, pp.442-449, Jun. 1988.

[29] H. H. Pennes, "Analysis of tissue and arterial blood temperatures in resting forearm," *J. Appl. Physiol.*, vol.1, pp.93-122, 1948.

[30] R. G. Gordon, R. B. Roemer, and S. M. Horvath, "A mathematical model of the human temperature regulatory system—transient cold exposure response," *IEEE Trans. Biomed. Eng.*, vol.23, pp.434–444, 1976.

[31] P. Bernardi, M. Cavagnaro, S. Pisa, and E. Piuzzi, "Specific absorption rate and temperature elevation in a subject exposed in the far-field of radio-frequency sources operating in the 10-900-MHz range," *IEEE Trans. Biomed. Eng.*, vol.50, no.3, pp.295-304, Mar. 2003.

[32] A. Hirata and O. Fujiwara, "Modeling time variation of blood temperature in the bioheat equation and its application to temperature analysis due to RF exposure," *Phys. Med. Biol*., vol.54, pp.N186-N196, 2009.

[33] P. J. Riu, K. R. Foster, D. W. Blick, and E. R. Adair, "A thermal model for human thresholds of microwave-evoked warmth sensation," *Bioelectromagnet.*, vol.18, no.8, pp.578-583, 1998.

Akimasa Hirata (S'99-M'01) received the B.E., M.E., Ph.D degrees in communication engineering from Osaka University, Suita, Osaka, Japan, in 1996, 1998, and 2000, respectively. He was a research fellow of the Japan Society for the Promotion of Science (JSPS Research Fellow) for the 1999-2001 period and also a visiting research scientist in the University of Victoria, Canada from May to October in 2000. In 2001, he joined the Department of Communication Engineering, Osaka University as an Assistant Professor. In 2004, he joined the Department of Computer Science and Engineering, Nagoya Institute of Technology as an Associate Professor. His research interests are in electron beam devices for high-power millimeter or sub-millimeter generation, bioelectromagnetics, waveguide analysis, EMC and EMI in power line, and computational techniques in electromagnetics.

Masami Kojima received his Ph. D. in 1991 from Kanazawa Medical University. He is an Associate Professor of Kanazawa Medical University. He was an Alexander von Humboldt Research Fellow in the department of Experimental Ophthalmology, University of Bonn, Germany from 1988 to 1990. His research interests focus on the mechanisms of cataract development in the lens. Currently he is working in the field of non-ionizing exposure such as ultraviolet, infra-red, and microwave and millimeter wave exposure related ocular damages.

Hiroki Kawai (S'01–M'05) received the B.E., M.E., and D.E. degrees in electrical engineering from Chiba University, Chiba, Japan, in 1999, 2001, and 2005, respectively. He is currently an Expert Researcher with the National Institute of Information and Communications Technology, Tokyo, Japan. His main interests include analysis and design of small antennas using animal study, research on evaluation of the interaction between electromagnetic fields, and the human body using numerical and experimental phantoms.

Yoko Yamashiro received BS degree in 1991 from Toyama University, Toyama, Japan. She is a PhD candidate at the same university and also a researcher of Kanazawa Medical University and. Her research interest includes cataract, and epidemiology and the influence of ultraviolet rays and electromagnetic waves on eyes.

Soichi Watanabe (S'93--M'96) received the B.E., M.E., and D.E., degrees in electrical engineering from Tokyo Metropolitan University, Tokyo, Japan, in 1991, 1993, and 1996, respectively. He is currently with the National Institute of Information and communications Technology (NICT), Tokyo, Japan. His main research interest is biomedical electromagnetic compatibility. Dr. Watanabe is a member of the Institute of Electronics, Information and Communication Engineers (IEICE), Japan, the Institute of Electrical Engineers (IEE), Japan, and the Bioelectromagnetics Society. Since 2004, he has also been a member of the Standing Committee on Physics and Engineering of the International Commission on Non-Ionizing Radiation Protection (ICNIRP). He was the recipient of several awards, including the 1996 International Scientific Radio Union (URSI) Young Scientist Award, the 1997 IEICE Best Paper Award, and the 2005 Roberts Prize of Physics in Medicine and Biology.

Hiroshi Sasaki received the B.S. degree in medicine from Kanazawa University, Kanazawa, Japan, in 1987. From 1987 to 1991 he was a resident physician in Jichi Medical University, Utsunomiya, Japan. For the period 1991-1993 he worked as a research fellow at Eye Research Institute, Oakland University, USA. He received his Ph.D. degree in medical science from Jichi Medical University, Japan in 1996. In 1996 he joined the Department of Ophthalmology, Kanazawa Medical University, Uchinada, Japan, as a lecturer and since 2005 he has been a professor and chairman in the department. His main research themes include cataract, epidemiology and the influence of ultraviolet rays and electromagnetic waves on eyes.

Osamu Fujiwara (M'84) received his B.E. degree in electronic engineering from Nagoya Institute of Technology, Nagoya, Japan, in 1971, and his M.E. and D.E. degrees in electrical engineering from Nagoya University, Nagoya, Japan, in 1973 and in 1980, respectively. From 1973 to 1976, he worked in the Central Research Laboratory, Hitachi, Ltd., Kokubunji, Japan, where he was engaged in research and development of system packaging designs for computers. From 1980 to 1985, he was a Research Associate and Assistant Professor in the Department of Electrical Engineering at Nagoya University. In 1985, as an Associate Professor, he joined the Department of Electrical and Computer Engineering of Nagoya Institute of Technology. Since 1993, he has been a Professor in the Department of Computer Science and Engineering, Graduate School of Engineering, Nagoya Institute of Technology. His research includes computational bioelectromagnetics, numerical dosimetry in human body and exposure assessment, in addition to electromagnetic compatibility (EMC).